Eur. Phys. J. B **18**, 601–604 (2000)

THE EUROPEAN PHYSICAL JOURNAL B

EDP Sciences

Appearance of anisotropic non s-wave superconductivity above the critical pressure of antiferromagnetic $CeRhIn_5$

^{115}In nuclear quadrupole resonance study

Y. Kohori[a], Y. Yamato, Y. Iwamoto, and T. Kohara

Department of Material Science, Faculty of Science, Himeji Institute of Technology, Kamigori-cho Ako-gun Hyogo 678-1297, Japan

Received 5 July 2000

Abstract. We have carried out ^{115}In nuclear quadrupole resonance (NQR) measurements in $CeRhIn_5$. At ambient pressure, $CeRhIn_5$ undergoes an antiferromagnetic AF phase transition at $T_N = 3.8$ K. The ^{115}In NQR spectrum has shown the appearance of a small internal field in the direction perpendicular to the tetragonal c-axis. With application of a hydrostatic pressure, the AF state is suppressed and the superconductivity appears just above the critical pressure ($P = 17$ kbar). The nuclear spin lattice relaxation rate $1/T_1$ of ^{115}In measured at $P = 27$ kbar indicates the occurrence of the superconductivity in the nearly AF region. In the superconducting state, $1/T_1$ has no Hebel-Slichter coherence peak just below T_c of 2 K and has a power law T-dependence (T^3) down to 300 mK. This is consistent with anisotropic superconductivity, with line nodes in the superconducting energy gap: non-s-wave superconductivity occurs in $CeRhIn_5$.

PACS. 74.20.Mn Nonconventional mechanisms (spin fluctuations, polarons and bipolarons, resonating valence bond model, anyon mechanism, marginal Fermi liquid, Luttinger liquid, etc.) – 71.27.+a Strongly correlated electron systems; heavy fermions – 76.60.Gv Quadrupole resonance

1 Introduction

The relation between magnetism and superconductivity is an important theme of heavy fermion system. Several years ago, $CeCu_2Si_2$ [1] and $CeCu_2Ge_2$ (at high pressures) [2] were the only superconducting members of the $4f$-heavy fermion metals. Since 1995, however, $CePd_2Si_2$ [3,4], $CeRh_2Si_2$ [5] $CeIn_3$ [6] and $CeNi_2Ge_2$ [7] have all been shown to be superconducting under pressure P. Except for $CeCu_2Si_2$, these compounds have an antiferromagnetic AF ground state at ambient pressure. The superconductivity located near the AF state has become one of the fundamental issues in condensed matter physics. Analogy with the high T_c cuprate superconductors suggests that the d-wave superconductivity mediated *via* AF spin fluctuations is realized in these compounds.

Recently, $CeRhIn_5$, which has the tetragonal $HoCoGa_5$ structure and can be viewed as alternating layers of $CeIn_3$ and $RhIn_2$ stacked sequentially along the tetragonal c-axis, has been discovered [8]. At ambient pressure, the ground state is antiferromagnetic with a Néel temperature, T_N, of 3.8 K. Application of a hydrostatic pressure of about 17 kbar induces a first-order-like transition to the superconducting state with the critical temperature T_c of 2.2 K, which is the highest among the pressure induced heavy fermion superconductors. The superconductivity occurred in the relatively low P and high T region in $CeRhIn_5$, which is suitable for microscopic measurements.

Nuclear magnetic resonance (NMR) and nuclear quadrupole resonance (NQR) are powerful methods for the study of magnetism and superconductivity, *i.e.*, the spectrum and the nuclear spin lattice relaxation rate, $1/T_1$, provide valuable information on the magnetic structure, the fluctuations of the moments and also the superconducting energy gap. There are two non-equivalent In sites in $CeRhIn_5$. One site is located in the Ce-In plane. This In site is surrounded by Ce ions and has a symmetry which is invariant under fourfold rotation (we hereafter referred to as site A in this paper). The other site is surrounded by Ce and Rh ions and has lower crystal symmetry (referred to as site B). Due to the non-cubic environment, one expects a large electric field gradient for both In sites, which is favorable for observing distinct NQR lines. In this paper, we report the study of ^{115}In NQR in $CeRhIn_5$ at ambient pressure and at the pressure of 27 kbar.

[a] e-mail: kohori@sci.himeji-tech.ac.jp

2 Experiment

The NQR measurements were performed using a phase-coherent pulsed NMR/NQR spectrometer in the resonance frequency range between 5–90 MHz. The value of T_1 was obtained by the recovery of the nuclear magnetization after a saturation pulse. The measurements above 1.3 K were performed using a ^{4}He cryostat, and below 1.3 K with a ^{3}He-^{4}He dilution refrigerator ($P = 27$ kbar) and a ^{3}He cryostat (ambient pressure). Polycrystalline $CeRhIn_5$ was synthesized by arc melting, subsequently annealing at 650 °C for a week, and then crushed into coarse powder with a diameter larger than 100 μm for the NQR measurement. The pressure up to 27 kbar was applied by a conventional BeCu/maraging steel piston and cylinder cells, filled with a mixture of Fluorinert 70 and 77. The magnitude of the pressure was determined by the superconducting transition of Sn [9].

3 Results and discussion

3.1 NQR spectrum

The onset temperature of the superconductivity in $CeRhIn_5$ measured by AC susceptibility does not change for P values from 17 kbar to 27 kbar. The transition is broad at 17 kbar and its width decreases rapidly with increasing P. The observed P-dependence of the superconductivity in $CeRhIn_5$ is different from that of $CeIn_3$ in which a very narrow superconducting P-region exists. Hence we performed ^{115}In NQR at 27 kbar for the study of superconductivity.

Figure 1a shows the ^{115}In NQR spectrum in the paramagnetic state ($T = 4.2$ K) obtained at ambient pressure. The spectrum consists of 8 narrow lines. The spectrum could be assigned as the signals arising from two In sites. The electric quadrupole - Hamiltonian is written as

$$\mathcal{H}_Q = \frac{e^2qQ}{4I(2I-1)}\left[3I_z^2 - I(I+1) + \frac{\eta}{2}(I^{+2} + I^{-2})\right].$$

Here Q represents the nuclear quadrupole moment, the electric-field gradients are contained in eq and the asymmetric parameter η, defined as $eq = V_{zz}$, and $\eta = (V_{xx} - V_{yy})/V_{zz}$. Conventionally, V_{zz} has the largest magnitude, and V_{xx} and V_{yy} are chosen so that $0 \leq \eta \leq 1$. For I= 9/2 (^{115}In), the four "allowed" transitions would be observed when η is small.

A set of lines observed at 6.8, 13.5, 20.4 and 27.1 MHz are equally separated, which represents $\eta = 0$. The signals arise from the site A (In atoms in Ce-In plane) which has axial electric field gradient. From the crystal structure, it is evident that the direction of the electric field gradient V_{zz} is in the tetragonal c-axis. The magnitude of the electric field gradient was found to be $e^2qQ/h = 163$ MHz. The other signals observed at 30.8, 34.2, 47.9 and 65.6 MHz could be assigned to be $e^2qQ/h = 400$ MHz and $\eta = 0.45$. The associated "forbidden" transition ($|\Delta m| > 1$), which exists in the case of finite η, was not visible. These signals arise from site B (^{115}In surrounded by Ce and Rh ions). Since symmetry of the electric field gradient in this site is lower than uniaxal, the principal axes of the electric field gradient tensor could not be determined only from NQR, but also the NMR measurement using a single crystal would be required. The system undergoes an AF phase transition at $T_N = 3.8$ K. Figure 1b shows the spectrum in the AF state ($T = 1.3$ K). For the signals from site A, the higher frequency resonance lines at 20 and 27 MHz remain nearly at the same frequencies, however, the lower frequency lines split and broaden. This change reflects the appearance of a small internal field H_{int} with the direction perpendicular to V_{zz}. The internal field with the magnitude of 1.8 kOe explains the approximate peak position of the broadened lines, as shown by arrows in Figure 1b. The broadening of lines could be explained by an inhomogeneous distribution of H_{int} of about 10%. As the direction of V_{zz} is the c-axis for site A, this spectrum indicates that H_{int} is parallel to the Ce-In plane. Such an internal field is induced by the Ce moments oriented perpendicular to the c-axis. The spectrum from the site B has a larger change in the AF state than that from site A, and only the highest frequency resonance line remains at the same frequency. The analysis of the spectrum is not simple, and requires

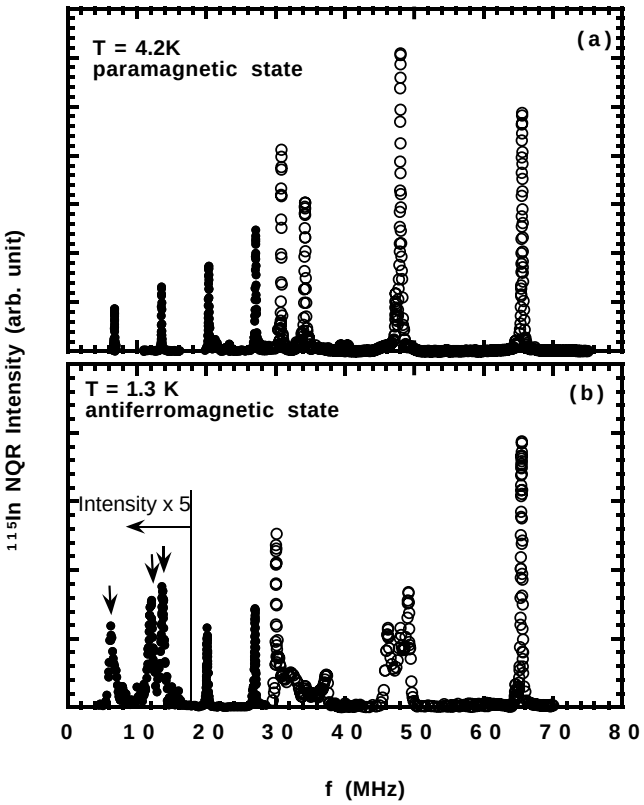

Fig. 1. ^{115}In NQR spectra obtained in paramagnetic state (a) and AF state (b). The closed circles represent the signals from site A, and open circles represent those from site B. Internal field with the magnitude of 1.8 kOe splits the lower frequency lines from site A. Calculated resonance frequencies are shown by arrows.

Table 1. *b*-coefficients for two different NQR transitions for $\eta = 0$ and 0.45, respectively.

η	transition	b_1	b_2	b_3	b_4
0	$\pm3/2 \leftrightarrow \pm5/2$	0.0303	0.1399	0.0242	0.8056
	$\pm7/2 \leftrightarrow \pm9/2$	0.1212	0.5594	0.2970	0.0224
0.45	$\pm3/2 \leftrightarrow \pm5/2$	0.0265	0.0439	0.0961	0.836
	$\pm7/2 \leftrightarrow \pm9/2$	0.1104	0.3694	0.4322	0.0880

information about the magnetic structure obtained from the neutron diffraction experiments, which has not been reported yet.

3.2 $1/T_1$ at ambient pressure

The nuclear spin-lattice relaxation rate was measured for both sites. For site A, the analysis is strict due to the axial symmetry of the electric field gradient. The expected functional form for $m(t)$ for spin $I = 9/2$, is a sum of four exponents with the coefficients determined by the initial conditions [10]. The function $m(t)$ thus contains only two fitting parameters, $1/T_1$ and numerical factor C, and is given by

$$1 - \frac{m(t)}{m(\infty)} = C\left[b_1 \exp\left(-\frac{3t}{T_1}\right) + b_2 \exp\left(-\frac{10t}{T_1}\right) + b_3 \exp\left(-\frac{21t}{T_1}\right) + b_4 \exp\left(-\frac{36t}{T_1}\right)\right].$$

In the course of our work we studied two different quadrupolar transitions $\pm3/2 \leftrightarrow \pm5/2$ (13.5 MHz) and $\pm7/2 \leftrightarrow \pm9/2$ (27 MHz). For these cases, the *b*-coefficients are given in Table 1. For site B, the analysis is complicated due to the non-axial electric field gradient. The extension to the finite η case has been performed, which shows the relaxation function changes with η [11]. When the relaxation occurs *via* an isotropic hyperfine coupling (such as Fermi-contact or core-polarization interaction) and the spin fluctuations are isotropic, the function form of $m(t)$ for $\eta = 0.45$ is expressed as,

$$1 - \frac{m(t)}{m(\infty)} = C\left[b_1 \exp\left(-\frac{3t}{T_1}\right) + b_2 \exp\left(-\frac{8.57t}{T_1}\right) + b_3 \exp\left(-\frac{16.65t}{T_1}\right) + b_4 \exp\left(-\frac{30.02t}{T_1}\right)\right],$$

where respective *b*-coefficients are also given in Table 1. In NQR, resonance frequency and relaxation function change smoothly with η. In this paper, the $\pm3/2 \leftrightarrow \pm5/2$ transition for finite η just means that the transition corresponds to $\pm3/2 \leftrightarrow \pm5/2$ transition for $\eta = 0$. We performed the analysis of the recovery curve with the above equations for site B, and obtained good fittings to the recovery curve.

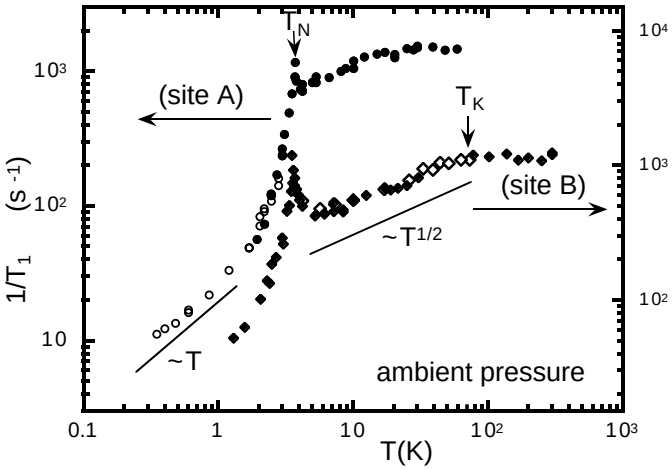

Fig. 2. Temperature dependence of $1/T_1$ at ambient pressure. The crossover from heavy fermion state to incoherent Kondo state occurs around T_K of 80 K. The solid lines have slopes of 1/2 and 1, which are guides to the eye for the T-dependence of $1/T_1$.

The T-dependence of $1/T_1$ for sites A and B obtained at ambient pressure is shown in Figure 2. The solid and open circles indicate the values measured at 13.5 MHz and 27 MHz for site A, and the solid and open diamonds indicate the values obtained at 30 MHz and 65 MHz for site B, respectively. In the paramagnetic state, there is no T-region, in which $1/T_1$ varies in proportion to T, as expected in the Fermi liquid state. $1/T_1$ varies nearly $\sqrt{T}$ up to 70–80 K for site B. Around $T_N = 3.8$ K, $1/T_1$ is markedly enhanced with a distinct peak, reflecting a critical slowing down of the fluctuations of Ce moments at T_N. The T-dependence of $1/T_1$ for site B is well explained by the theory developed for the electronic states around the antiferromagnetic instabilities [12,13]. The enhancement is larger in site B than that in site A at T_N. Due to the form factor of hyperfine coupling to the neighboring Ce spins, the critical phenomenon at T_N is suppressed at site A. With decreasing T below T_N, $1/T_1$ decreases rapidly for both sites, and approaches a $T_1T =$ const. law below 1 K (site A). Above 80 K, $1/T_1$ becomes T-independent up to 300 K, indicating that a crossover occurs from the heavy fermion state at low T to the incoherent Kondo scattering state at high T.

3.3 $1/T_1$ at high pressure

Figure 3 shows $1/T_1$ measured under high pressure. At 27 kbar, AF order disappears and $1/T_1$ in the paramagnetic state is also strongly suppressed from the value at ambient pressure for both sites. However, $1/T_1$ still varies proportionally to $\sqrt{T}$. This result indicates that the system remains in a nearly AF state in which the superconductivity appears. For site A, $1/T_1$ was measured down to 0.3 K. $1/T_1$ is markedly reduced below 2.0 K. The value of T_c obtained from $1/T_1$ is slightly lower than the value

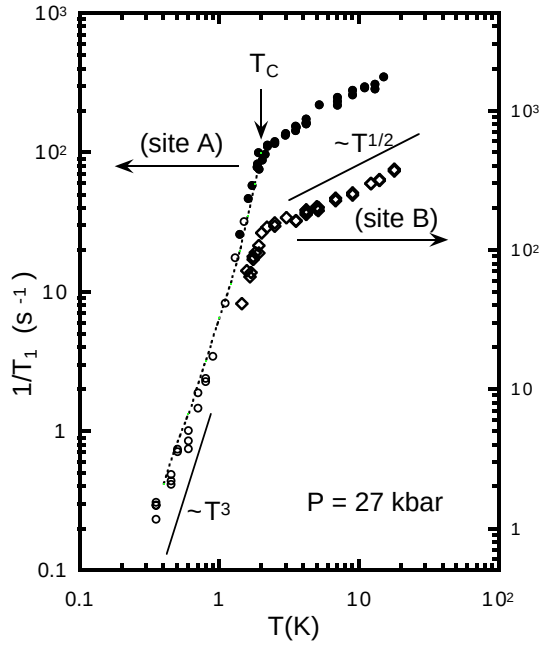

Fig. 3. Temperature dependence of $1/T_1$ at $P = 27$ kbar. The solid lines have slopes of 1/2 and 3, respectively.

measured by AC susceptibility. As ^{115}In NQR measurement was performed in coarse powder, T_c might be reduced slightly by the defects induced by sample preparation. There is no Hebel-Slichter coherence peak just below T_c, and $1/T_1$ varies in proportion to T^3 at very low temperatures, which is reminiscent of the relaxation behavior in heavy fermion superconductors reported so far [14]. The behavior of $1/T_1$ in the superconducting state of $CeRhIn_5$ provides an evidence for an unconventional nature of the superconductivity. The result shows that the gap is anisotropic suggesting non-s-wave (probably d-wave) superconductivity being realized in this system owing to a strong on-site repulsion. If we try to calculate T_1 tentatively assuming $\Delta = \Delta_0 \cos\theta$ with $2\Delta_0(T = 0) = 8\, k_B T_c$, experimental values are reproduced well as plotted by dotted line in Figure 3 ($1/T_1$ is well interpreted by an anisotropic energy gap model with gap zeros on the lines at the Fermi surface).

4 Summary

We determined from ^{115}In NQR that the AF state in $CeRhIn_5$ was located close to the non-magnetic boundary. Above the critical P, $1/T_1$ has no enhancement just below T_c and a T^3 dependence at low temperature, which provides evidence for an unconventional nature of the superconductivity.

This work was supported by a grant-in-aid from the Ministry of Education, Science and Culture of Japan.

References

1. F. Steglich, J. Aarts, C.D. Bredl, W. Lieke, D. Meschede, W. Franz, H. Schafer, Phys. Rev. Lett. **43**, 1892 (1979).
2. D. Jaccard, K. Behnia, J. Sierro, Phys. Lett. A **163**, 475 (1992).
3. F.M. Grosche, S.R. Julian, N.D. Mathur, G.G. Lonzarich, Physica B **224**, 50 (1996).
4. F.M. Grosche, S.R. Julian, N.D. Mathur, F.V. Carter, G.G. Lonzarich, Physica B **237**, 197 (1997).
5. R. Movshovich, T. Graf, D. Mandrus, J.D. Thompson, J.L. Smith, Z. Fisk, Phys. Rev. B **53**, 8241(1996).
6. I.R. Walker, F.M. Grosche, D.M. Freye, G.G. Lonzarich, Physica C **282**, 303 (1997).
7. S.J.S. Lister, F.M. Grosche, F.V. Carter, R.K.W. Haselwimmer, S.S. Saxena, N.D. Mathur, S.R. Julian, G.G. Lonzarich, Z. Phys. B **103**, 263 (1997).
8. H. Hegger, C. Petrovic, E.G. Moshopoulou, M.F. Hundley, J.L. Sarrao, Z. Fisk, J.D. Thompson, Phys. Rev. Lett. **84**, 4986 (2000).
9. T.F. Smith, C.W. Chu, M.B. Maple, Cryogenics **9**, 53 (1969).
10. D.E. MacLaughlin, J.D. Williamson, J. Butterworth, Phys. Rev. B **4**, 60 (1971).
11. J. Chepin, J.H. Ross Jr, J. Phys. Cond. Matt. **3**, 8103 (1991).
12. A. Ishigaki, T. Moriya, J. Phys. Soc. Jpn **65**, 3402 (1996).
13. T. Moriya, K. Ueda, Solid State Commun. **15**, 169 (1974).
14. For example, Y. Kohori K. Matsuda, T. Kohara, Hyperfine Interact. **120/121**, 503 (1999).